New Transceiver Scheme for FDMA Systems Based on Discrete Sine Transform

BASHAR ALI FAREA AND NOR SHAHIDA MOHD SHAH
Department of Communication Engineering,
University Tun Hussein Onn Malaysia
Parit Raja, Batu Pahat, Johor
Malaysia
* shahida@uthm.edu.my,eng.bashar2@yahoo.com

Abstract: - In this paper, the discrete sine transform (DST) as an orthogonal basis is used rather than the conventional discrete Fourier transform (DFT) to implement the orthogonal frequency division multiple access (OFDMA) system. The obtained system is called a DST-OFDMA system. The performance of the proposed DST-OFDMA system is studied and compared with the conventional discrete Fourier transform (DFT)-based OFDMA (DFT-OFDMA) system. The peak power problem in the proposed DST-OFDMA and in the recent DST-based SC-FDMA (DST-SC-FDMA) is also investigated and compared for different subcarriers mapping schemes and modulation formats. The impact of the radio resources allocation is also investigated at different roll-off factors. Simulation results show the improvement in the bit error rate (BER) of the proposed system over the conventional system by about 9 dB and 6 dB for interleaved and localized subcarriers mapping, respectively with quadrature phase shift keying (QPSK).

Key-Words: - DST, OFDMA, SC-FDMA, DFT, PAPR, BER.

1. Introduction

In the past few years, the orthogonal frequency division multiple access (OFDMA) system had gained more attention since it has high spectral efficiency, robustness to multipath fading, and immunity against inter-symbol interference (ISI). Currently, it is used in wireless local area network (LAN) and broadband wireless access. As a result, it has been chosen as a downlink transmission technique in third generation partnership project long-term evaluation (3GPP LTE) standards [1]. However, OFDMA system suffers from a high peak-to-average power ratio (PAPR) problem. This critical issue leads to high power consumption, inband distortion, and spectrum spreading when the OFDMA signal passes through a nonlinear power amplifier [2]. Recently, single-carrier frequency division multiple access (SC-FDMA) system has received a lot of attention for its advantages such as low PAPR and low sensitivity to carrier frequency offsets [1-5]. These advantages motivate the manufacturers to introduce this system in the uplink of 3GPP LTE and 3GPP LTE advanced. Various methods are available to map the subcarriers in the FDMA systems. However, the commonly used methods are Interleaved FDMA (IFDMA) and Localized FDMA (LFDMA) [6]. In IFDMA, the output data corresponding to a single user are allocated to equidistant subcarriers over the entire bandwidth. In LFDMA, the output data are allocated to consecutive subcarriers [2].

In the literature, the discrete Fourier transform (DFT) as an orthogonal basis to implement the SC-FDMA and OFDMA systems were extensively studied and many techniques were proposed to reduce the PAPR [1, 2, 4, 6-9]. However, a few works had been done on the trigonometric implementation of the FDMA systems. The discrete cosine transform (DCT) based OFDMA (DCT-OFDMA) was proposed to implement FDMA systems and reduce the PAPR [10-12].

The discrete sine transform (DST) based OFDMA (DST-OFDMA) is not studied so far and only a few works had been done on DST to implement the SC-FDMA system [13-14]. DST uses only real functions instead of the complex functions (exponential functions) used in the conventional DFT. As a result, the complexity of the signal processing, and the in-phase/quadrature imbalance I/Q) is reduced [15, 16]. Therefore, our proposed technique which DST to implement the FDMA systems demonstrates clear advantages over DFT.

In this paper, the DST is proposed as orthogonal basis to implement the OFDMA system thereby the transceiver scheme uses a DST rather than the DFT. The scheme is described and its model is derived. The BER of the proposed DST-OFDMA scheme is presented and compared with the previous system DFT-OFDMA. Moreover, the PAPR performances of the proposed DST-OFDMA system is studied and compared with recent DST-SC-FDMA system for different subcarrier mapping and modulation formats. In contrast to the conventional DFT-OFDMA system, it is found that DST-OFDMA provides good BER performance and an acceptable PAPR performance especially with interleaved mapping.

The rest of this paper is organized as follows: Section 2 introduces a mathematic model of the proposed DST-OFDMA system. Section 3 describes the recent DST-SC-FDMA system. The time domain symbols of proposed scheme is driven in section 4. The PAPR problem is discussed in section 5. Section 6 deals with Pulse-shaping filter. Simulation results are given in Section 7. Finally, Section 8 concludes the paper.

2. The Proposed DST-OFDMA System

The exponential function of the DFT consists of two parts, real parts (cosine) and imaginary parts (sine). These parts can be represented mathematically as a Fourier-related transform and so called the discrete cosine transform (DCT) and the discrete sine transform (DST) with a purely real matrix. The DST is given by [9].

$$Y(k) = \sqrt{\frac{2}{N+1}} \sum_{n=0}^{N-1} \mathrm{x(n)} \left(\sin\pi \frac{(k+1)(n+1)}{N+1} \right), \quad k = 1,2.,N \tag{1}$$

The inverse DST (IDST) is given by

$$\mathrm{X(n)} = \sqrt{\frac{2}{N+1}} \sum_{k=0}^{N-1} \mathrm{Y(k)} \left(\sin\pi \frac{(k+1)(n+1)}{N+1} \right), \quad n = 1,2.,N \tag{2}$$

Where x(n) and Y(k) are the signal in the time and frequency domains, respectively. N is the number of subcarriers. In our proposed scheme a single set of sinusoidal functions DST is used instead of exponential functions DFT. Figures 1 presents the transceiver block diagrams of the DST-OFDMA systems. The encoding process is performed for input stream as a first step at the transmitter side then the modulation process takes place to map the coded bits to multilevel symbols using different modulation formats such as quadrature phase shift keying (QPSK) and 16-quadrature amplitude modulation (16QAM). After modulation, the symbols are grouped into N symbols and forward directly to the subcarrier mapping block to assign the DST outputs into M subcarriers that can be transmitted. After performing an M-point IDST, a cyclic prefix (CP) is added to the transmitted block and the signal can express as follows:

$$\bar{\bar{\mathbf{x}}}_{\mathbf{u}} = \mathbf{P}\, \mathbf{S}_{\mathbf{M}}^{-\mathbf{1}} \coprod_{\mathbf{T}}^{\mathbf{u}} \bar{\mathbf{x}}_{\mathbf{u}} \tag{3}$$

Where $\bar{\mathbf{x}}_{\mathbf{u}}$ is a vector of size N × 1 denoted to the user's modulated symbols. $\mathbf{S}_{\mathbf{N}}$ is a DST matrix of size N×N and $\coprod_{\mathbf{T}}^{\mathbf{u}}$ is a subcarriers mapping technique with M × N matrix size. An IDST matrix of size M×M is denoted by $\mathbf{S}_{\mathbf{M}}^{-\mathbf{1}}$. M = Z·N and the systems can handle Z simultaneous users without co-channel interference (CCI). P is a CP of matrix size (M+ L) ×M and length L. The representation of $\coprod_{\mathbf{T}}^{\mathbf{u}}$ for both the localized and the interleaved techniques can be expressed in (4) and (5), respectively

$$\coprod_{\mathbf{T}}^{\mathbf{u}} = \left[\mathbf{0}_{(u-1)N\times N}; \boldsymbol{I}_{\boldsymbol{N}}; \mathbf{0}_{(M-uN)\times N}\right] \tag{4}$$

$$\coprod_{\mathbf{T}}^{\mathbf{u}} = \left[\mathbf{0}_{(u-1)\times N}; \boldsymbol{u}_1^T; \mathbf{0}_{(Z-1)\times N}; \ldots; \mathbf{0}_{(u-1)\times N}; \boldsymbol{u}_N^T; \mathbf{0}_{(Z-u)\times N}\right] \tag{5}$$

Where the $\mathbf{I}_N$ is an N × N identity matrix and $\mathbf{0}_{(Z\times N)}$ is zero matrix of size Z×N, respectively. The CP matrix is given by

$$\mathbf{P} = [\boldsymbol{C}, \boldsymbol{I}_{\boldsymbol{M}}]^{\boldsymbol{T}} \tag{6}$$

Where

$$\mathbf{C} = \left[\mathbf{0}_{\mathrm{L}\times(\mathrm{M}-\mathrm{L}),}\mathbf{I}_{\mathrm{L}}\right]^{\mathbf{T}} \tag{7}$$

The reverse process occurs at the receiver side by removing the CP matrix and the received signal can be written as follow

$$\mathbf{r} = \sum_{\mathbf{u}=\mathbf{1}}^{\mathbf{U}} \mathbf{H}_{\mathbf{c}}^{\mathbf{u}}\, \bar{\bar{\mathbf{x}}}_{\mathbf{u}} + \mathbf{n} \tag{8}$$

Where $\bar{\bar{\mathbf{x}}}_{\mathbf{u}}$ are the transmitted symbols of vector M × 1. $\mathbf{H}_{\mathbf{c}}^{\mathbf{u}}$ is an M × M matrix describing the multipath channel matrix between the user and the base station. n is a vector of size M × 1 describing the additive noise. After applying DFT, the received signal can be written as follows:

$$\mathbf{R} = \sum_{\mathbf{u}=\mathbf{1}}^{\mathbf{U}} \mathbf{D}^{\mathbf{u}}\, \boldsymbol{\mathcal{F}}_{\boldsymbol{M}} \bar{\bar{\bar{\mathbf{X}}}}_{\mathbf{u}} + \mathbf{N} \tag{9}$$

Where, the diagonal matrix D^u is a DFT of a circulant sequence of $\mathbf{H_c^u}$ with M × M dimension. N and $\bar{\bar{\mathbf{X}}}_\mathbf{u}$ are the DFT of n and $\bar{\bar{\mathbf{x}}}_\mathbf{u}$, respectively. $\boldsymbol{\mathcal{F}_M}$ is a M× M DFT matrix. The FDE, the M-points IDFT, M-point DST, demapping subcarriers and the demodulation processes are implemented to estimate the modulated signal as follows:

$$\overleftrightarrow{\mathbf{X}}_\mathbf{u} = \coprod_{\mathbf{R}}^{\mathbf{u}} \ \mathbf{S_M}\, \boldsymbol{\mathcal{F}}_\mathbf{M}^{-\mathbf{1}}\, \mathbf{E_u}\, \mathbf{R} \qquad (10)$$

Where $\mathbf{E_u}$ and $\coprod_{\mathbf{R}}^{\mathbf{u}}$ are the M × M FDE matrix and N × M subcarrier demapper matrix, respectively. $\boldsymbol{\mathcal{F}}_\mathbf{M}^{-\mathbf{1}}$ and $\mathbf{S_M}$ are a M×M IDFT and DST matrixes, respectively. The throughput of the systems can be obtained after demodulation and decoding processes.

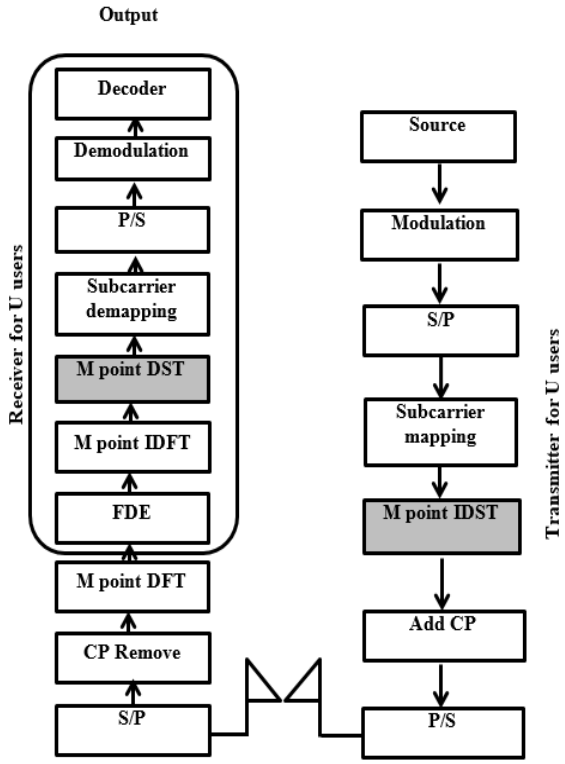

Fig.1: Transceiver structure of the DST-OFDMA system.

3. The Recent DST-SC-FDMA System

The recent DST-SC-FDMA system is discussed in [9]. Figure 2 depicts the transceiver of the recent DST-SC-FDMA system. It is more complex than our proposed scheme due to adding IDST block of at the transmitter side and DST block at the receiver side. As a result, the cost and computation complexity of the system are increased as well. However, it provides better performance in terms of PAPR. In the matrix notation the signal at the end of the transmitter can be expressed as follows:

$$\bar{\bar{\mathbf{x}}}_\mathbf{u} = \mathbf{P}\, \mathbf{S}_\mathbf{M}^{-\mathbf{1}} \coprod_{\mathbf{T}}^{\mathbf{u}} \mathbf{S_N}\, \bar{\mathrm{x}}_\mathrm{u} \qquad (11)$$

At the receiver side, all processes are performed to estimate the modulated symbols as follows:

$$\overleftrightarrow{\mathbf{X}}_\mathbf{u} = \mathbf{S}_\mathbf{N}^{-\mathbf{1}} \coprod_{\mathbf{R}}^{\mathbf{u}} \mathbf{S_M}\, \boldsymbol{\mathcal{F}}_\mathbf{M}^{-\mathbf{1}}\, \mathbf{E_u}\, \mathbf{R} \qquad (12)$$

The transmitted symbols can be obtained after demodulation and the decoding processes.

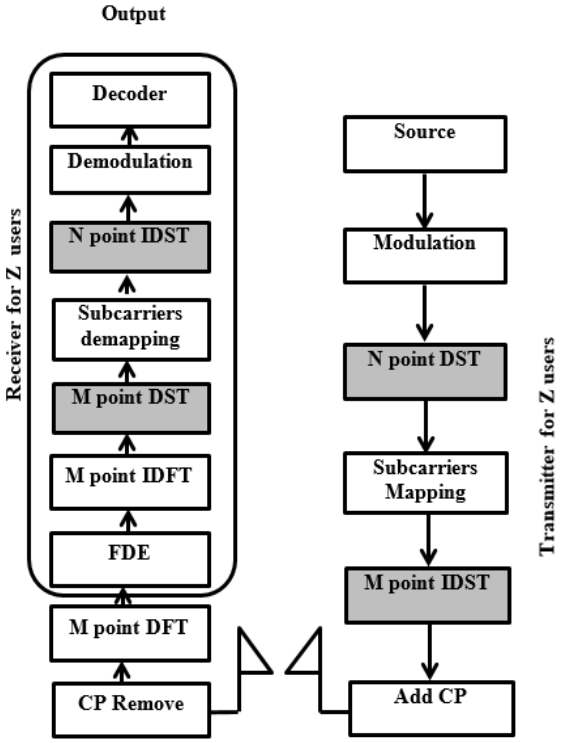

Fig.2: Transceiver structure of the DST-SC-FDMA system.

4. Time Domain Symbols of the DST-OFDMA System

In this section, the derivation of the time domain symbols is presented for the localized and interleaved subcarriers mapping techniques before applying the pulse shaping filter.

4.1 Time domain symbols of the interleaved DST- OFDMA system

The symbols after interleaved subcarriers mapping can be described as follows:

$$x(\bar{\mathrm{I}}) = \begin{cases} X(k) & \bar{\mathrm{I}} = Zk + z \\ 0 & Otherwise \end{cases} \qquad (13)$$

Applying IDST for the symbols after interleaved subcarrier mapping.

$$x(m) = \sqrt{\frac{2}{M+1}} \sum_{\bar{I}=0}^{M-1} X(\bar{I}) \sin\left(\frac{\eth(m+1)(\bar{I}+1)}{M+1}\right) \quad (14)$$

Use (13) in (14)

$$x(m) = \sqrt{\frac{2}{ZN+1}} \sum_{\bar{I}=ZK+z}^{M-1} X(k) * \sin\left(\frac{\pi(m+1)(Zk+z+1)}{ZN+1}\right) \quad (15)$$

$X(\bar{I})$ is represented the samples after the interleaved subcarrier mapping and $x(m)$ (m = 0, 1, . , M − 1) is the signal in the time domain after IDST.

$$x(m) = \sqrt{\frac{N+1}{ZN+1}} \sqrt{\frac{2}{N+1}} \sum_{k=0}^{N-1} X(k) * \sin\left(\frac{\pi(m+1)(k+1)(N+1)(Zk+z+1)}{(N+1) \quad (ZN+1)(k+1)}\right) (16)$$

After the IDST, output symbols are the same as the input symbols but with difference factor $\sqrt{(\mathrm{N}+1)/(\mathrm{M}+1)}$ and difference phase $(\mathrm{N}+1)(\mathrm{Zk}+\mathrm{z}+1)/(\mathrm{ZN}+1)(\mathrm{k}+1)$.
The fluctuation of the envelope of the time domain signal at the end of the transmitter depend on the variations in the phase and magnitude.

4.2 Time domain symbols of the localized DST-OFDMA system

The symbols after localized subcarriers mapping can be presented as follows:

$$x(\bar{I}) = \begin{cases} x(k) & \bar{I} = zN + k \\ 0 & \bar{I} = N, \ldots., M-1 \end{cases} \quad (17)$$

The symbols of the localized subcarriers mapping after IDST can be expressed as follows:

$$x(m) = \sqrt{\frac{2}{M+1}} \sum_{\bar{I}=0}^{M-1} X(\bar{I}) \sin\left(\frac{\pi(m+1)(\bar{I}+1)}{M+1}\right) \quad (18)$$

Use (17) in (18)

$$x(m) = \sqrt{\frac{2}{ZN+1}} \sum_{\bar{I}=k}^{M-1} X(k) * \sin\left(\frac{\pi(m+1)(zN+k+1)}{ZN+1}\right) \quad (19)$$

The (20) can be modified as follows:

$$x(m) = \sqrt{\frac{N+1}{ZN+1}} \sqrt{\frac{2}{N+1}} \sum_{k=0}^{N-1} X(k) * \sin\left(\frac{\pi(m+1)(k+1)}{(N+1)} \frac{(N+1)(zN+k+1)}{(ZN+1)(k+1)}\right) (20)$$

The output symbols after the IDST are the same as input symbols, but with differentiating factor $\sqrt{(\mathrm{N}+1)/(\mathrm{M}+1)}$, similar to that in the interleaved mapping, and difference phase $(N+1)(zN+k+1)/(ZN+1)(k+1)$.

5. Peak Power Problem

PAPR is defined as the ratio between the peak power and the average power of the transmitted signal. The PAPR against the complementary Cumulative distribution (CCDF) function in the FDMA systems is used to measure the effect of the peak power problem. CCDF is the probability that the PAPR is higher than a certain PAPR value (Pro (PAPR)> PAPR0) [9].

$$\mathrm{CCDF} = 1 - (1 - \mathrm{e}^{\mathrm{PAPR0}})^{\mathrm{N}} \quad (21)$$

where N is the number of subcarriers and the PAPR0 is a threshold. The PAPR is represented as follows

$$PAPR(dB) = 10.\log_{10}\left(\frac{\max\left(|x(m)|^2\right)}{\frac{1}{M}\sum_{m=0}^{M-1}|x(m)|^2}\right) \quad (22)$$

Where x(m) is the transmitted signal symbols.

6. Pulse-Shaping Filters

The rectangular pulses spread in time when they are pass through a band-limited channel, thereby caused inter-symbol interference (ISI). The pulse shaping techniques are used to simultaneously reduce the ISI and the spectral width of the modulated data. The impulse response of an RC filter is given by [10]

$$h(t) = \text{sinc}\left(\pi \frac{t}{T}\right) \frac{\cos\left(\pi\gamma \frac{t}{T}\right)}{1 - 4\left(\gamma \frac{t}{T}\right)^2} \qquad (23)$$

Where γ and T are the roll-off factor and the symbol period, respectively. The range of γ is {0,1}.

7. Simulation Results

7.1 Simulation Parameters

Simulation parameters which are used to study the performance (BER) and PAPR of the proposed DST-OFDMA and recent DST-SC-FDMA system are tabulated in table 1.

Table 1: Simulation parameters

Simulation method	Monte Carlo
Bandwidth	5 MHz
Modulation	QPSK and 16-QAM OFDMA
L	20 samples
M	512
N	128
Number of users	*M/N*=4
Subcarriers spacing	9.765625 KHz
Coding Method	Convolutional code with rate=1/2
Subcarriers mapping techniques	Localized and interleaved
Channel model	Vehicular A outdoor channel
Pulse shaping	Raised-cosine (RC)
Equalization	MMSE

7.2 BER performance

Figures 3 and 4 depict the BER performances for proposed DST-OFDMA system and conventional DFT-OFDMA system together with different subcarriers mapping techniques and modulation formats, QPSK and 16 QAM. It can be observed that the proposed DST-OFDMA system presents a significant BER performance improvement over the conventional DFT-OFDMA system for QPSK and 16-QAM. For QPSK and at BER=10^{-4} the improvement gain is approximately 9 dB for the DST-IOFDMA system, and 7 dB for the DST-LOFDMA system when compared to that of the DFT-IOFDMA and DFT-LOFDMA systems respectively. However, for two modulation formats QPSK and 16-QAM, the achievement of the interleaved mapping technique is better than the localized mapping technique for both systems DST-OFDMA and DFT-OFDMA, especially with the QPSK. In general, the performance of two systems in the modulation format QPSK is better in comparison with the high order modulation format 16-QAM.

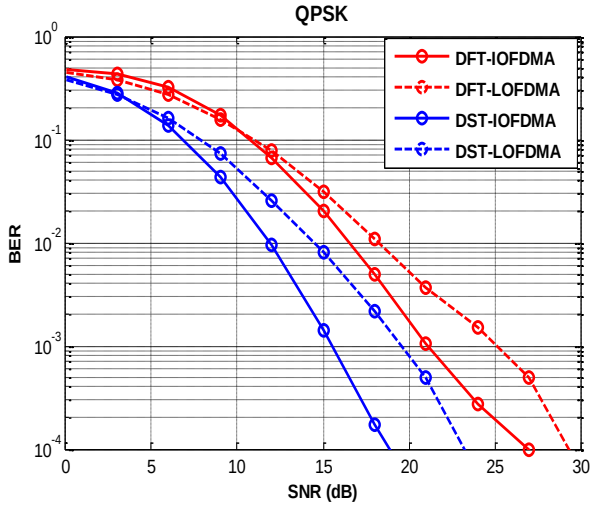

Fig.3: BER vs. SNR for the DFT-OFDMA and DST-OFDMA systems for different mapping techniques and QPSK.

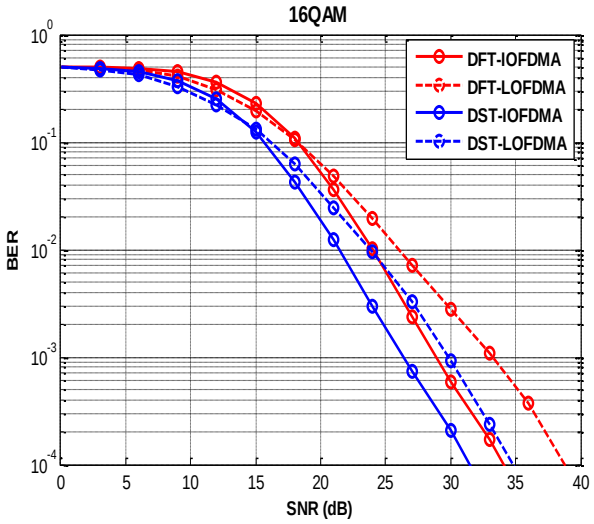

Fig.4: BER vs. SNR for the DFT-OFDMA and DST-OFDMA systems for different mapping mapping techniques and 16QAM.

7.3 PAPR Performance

7.3.1 The Effects of the Raised Cosine (RC) Filter

The PAPR with its CCDFs (Prob (PAPP>PAPR0)) for proposed DST-OFDMA, recent DST-SC-FDMA and conventional DFT-SC-FDMA systems is presented in the figures 5 and 6 for different subcarriers mapping techniques and modulation formats. The RC filter is not applied to the transmitter. It can be seen that the interleaved subcarriers mapping presents lower PAPR in the DST-SC-FDMA system than that in the DST-

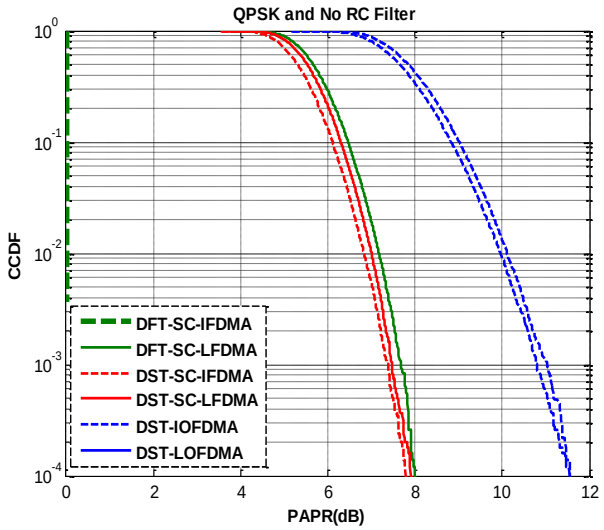

Fig.5: PAPRs and its CCDFs for the conventional DFT, recent DST and proposed DST-OFDMA systems with QPSK and no RC filter applied.

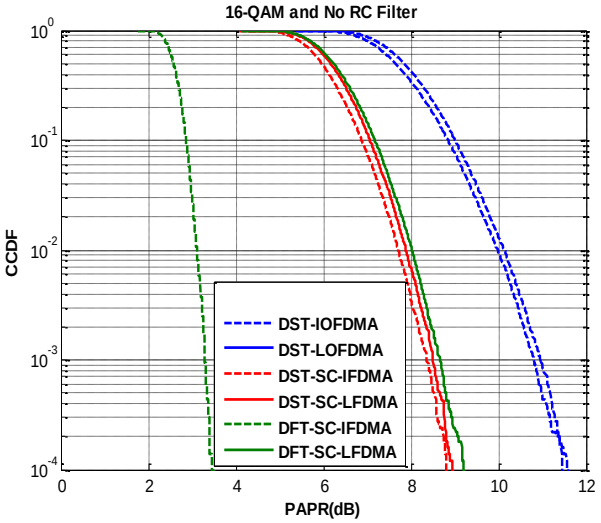

Fig.6: PAPRs and its CCDFs for the conventional DFT, recent DST and proposed DST-OFDMA systems with 16-QAM and no RC filter applied.

OFDMA system by approximately 4dB for QPSK and 2 dB for 16-QAM, but it increases over DFT-SC-FDMA system by 8 dB for QPSK and 6 dB for 16-QAM. In general, the different subcarriers mapping techniques do not affect largely on the PAPR performance for the DST-SC-FDMA and DST-OFDMA systems, regardless of the modulation formats, where the PAPR performance is nearly similar with the different subcarriers mapping techniques in each system. For the conventional DFT system, the different subcarriers mapping have large effects on the PAPR with different modulation formats. The effects of RC filter on the PAPR rendering for proposed DST-OFDMA, recent DST-SC-FDMA and conventional

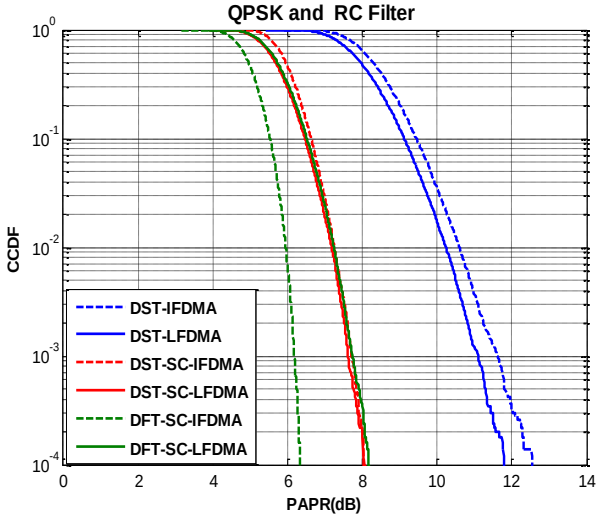

Fig.7: PAPRs and its CCDFs for the conventional DFT, recent DST and proposed DST-OFDMA systems with RC filter and QPSK.

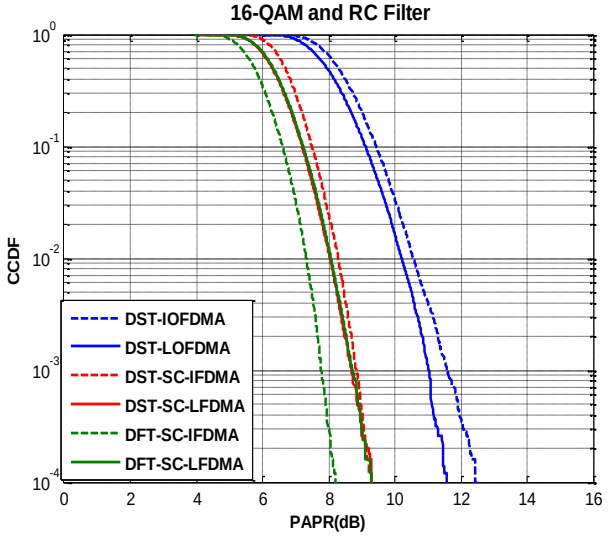

Fig.8: PAPRs and its CCDFs for the conventional DFT, recent DST and proposed DST-OFDMA systems with RC filter and 16-QAM.

DFT-SC-FDMA systems are demonstrated in the figures 7 and 8. γ = 0.22 is considered in the simulation. The increase of PAPR is noticeable for the proposed, recent DST, and conventional DFT systems where the increase in PAPR is about 0.4 dB and 1 dB for the DST-SC-IFDMA and the DST-IOFDMA for QPSK and 16-QAM, respectively. However, the rise in the DFT-SC-IFDMA system is 6.5 dB and 4.5 dB for QPSK and 16-QAM, respectively. In other words, the PAPR of the proposed and recent DST systems is insensitive to applying RC filter for different modulation types. At a CCDF = 10^{-3}, the PAPR is investigated and compared for different FDMA systems in the table 2.

Table 2: PAPRs at a CCDF = 10^{-3} for the conventional DFT, recent and proposed DST system

	QPSK		16-QAM	
Pulse-shaping	None (dB)	RC (dB)	None (dB)	RC (dB)
DST-SC-IFDMA	7.2	7.5	8.5	9
DST-SC-LFDMA	7.5	7.5	8.7	8.8
DST-IOFDMA	10.8	11.5	10.8	11.5
DST-LOFDMA	11	11	11	11
DFT-SC-IFDMA	0	6.2	3.3	7.8
DFT-SC-LFDMA	8	7.5	8.8	9

It is noticeable that the conventional DFT-SC-LFDMA system shows slight increase in PAPR over the DST-SC-LFDMA system, whereas the PAPR of the proposed DST-OFDMA system is demonstrated a clear increase over recent DST and conventional DFT systems but with low cost and complexity. There is a trade-off between the complexity and PAPR reduction in the proposed DST-OFDMA and recent DST-SC-FDMA schemes. Notably, the proposed scheme has a clear advantages over other systems such as in low cost, complexity, and less computation.

7.3.2 The Influence of the Resource Unit

Figures 9 through 12 present the influence of the resource unit on the PAPR of the proposed DST and recent DST systems with localized and interleaved subcarriers mapping techniques and QPSK modulation format. It can be seen that the influence of the resource unit has the same trend on the both systems that is the increase in the PAPR. It is also observed that a variation in the PAPR is a function of the radio resources allocation for both systems. In other words, a convolution process between random samples of the signal and the impulse response of the RC filter produces a signal with a high peak as γ values increased. In the same time, the out of band increases with γ values increase lead to high PAPR. The PAPR of RU#0 increases nearly uniformly with an increase in the values of γ from 0 to 1 for both the DST-SC-IFDMA and the DST-IOFDMA systems, whereas it is insensitive to roll-off increasing for both the DST-SC-LFDMA and the DST-LOFDMA systems. This effect can be explained in (16) and (20). For the first resource unit, RU#1, the PAPR increases with increase the values of γ for both systems. The RU#2 and RU#3 demonstrate highly increase in the PAPR when the values of γ increase for both proposed and recent DST systems. In general, for the both systems, the PAPR increases with the increase in roll-off factor. Table 3 depicts PAPRs for both DST systems with CCDF = 10-3 and γ = 0.35.

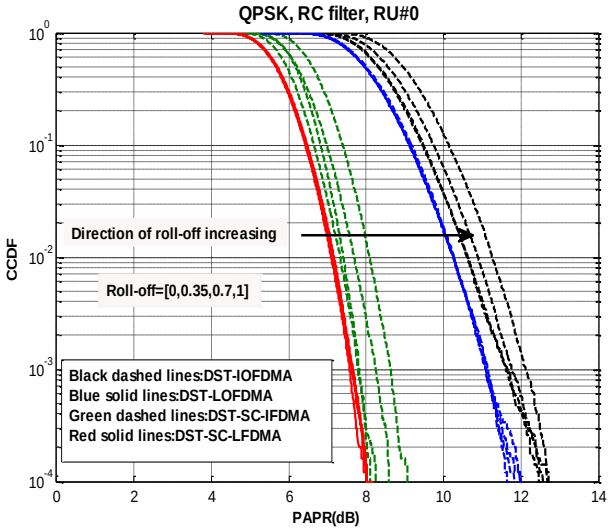

Fig.9: PAPRs and its CCDFs for the recent DST and proposed DST-OFDMA systems with RC filter and different values of γ for RU#0.

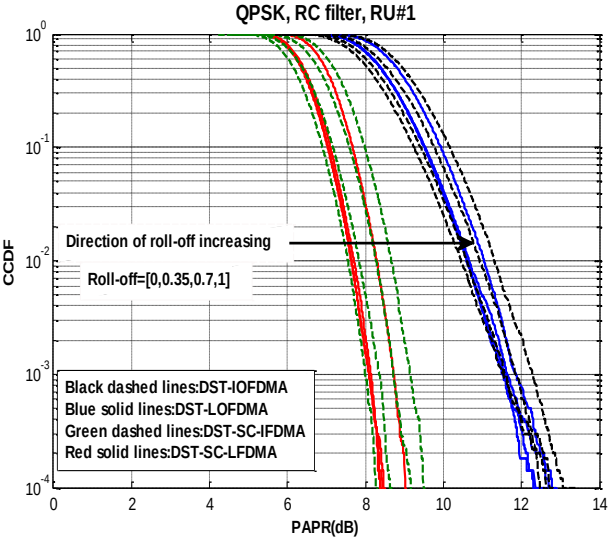

Fig.10: PAPRs and its CCDFs for the recent DST and proposed DST-OFDMA systems with RC filter and different values of γ for RU#1.

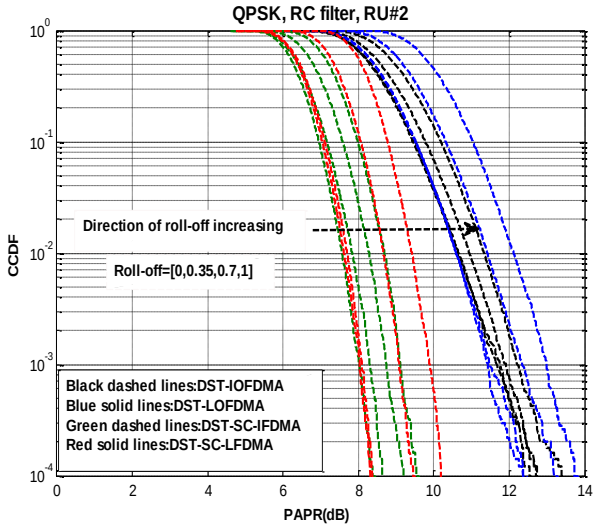

Fig.11: PAPRs and its CCDFs for the recent DST and proposed DST-OFDMA systems with RC filter and different values of γ for RU#2

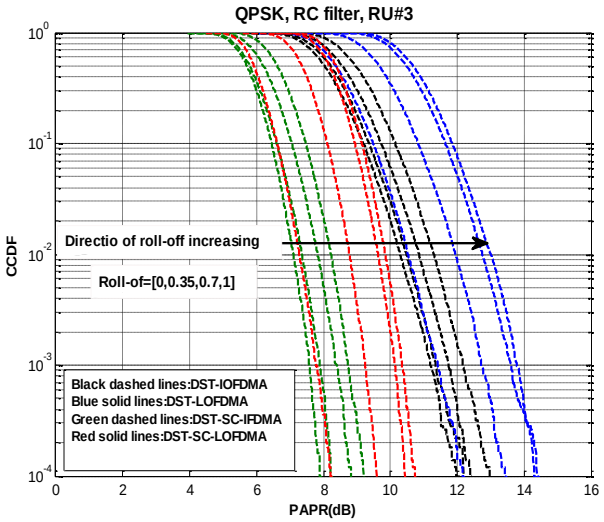

Fig.12: PAPRs and its CCDFs for the recent DST and proposed DST-OFDMA systems with RC filter and different values of γ for RU#3.

Table 3: PAPRs (in dB) at a CCDF = 10^{-3}, and γ = 0.35 for the DST base FDMA systems.

Mapping scheme	User 1	User 2	User 3	User 4
DST-SC-LFDMA	7.5	8	8	7.8
DST-SC-IFDMA	7.7	7.8	8	7.5
DST-LOFDMA	11	11.3	11.3	11.3
DST-IOFDMA	11.5	11.3	11.5	11

8. Conclusion

In this paper, an efficient transceiver scheme based on the DST for future wireless communications, namely DST-OFDMA has been introduced and investigated. The system model of the proposed DST-OFDMA system has been derived and its performance has been studied and compared with the conventional DFT-OFDMA system. Simulation results have been shown that the DST-OFDMA system provides superior BER improvement over the DFT-OFDMA system. The results have also been demonstrated that, by applying the RC filter, the PAPRs are reduced especially with the DFT-SC-IFDMA and the DST-IOFDMA systems. However, the influence of the resources unit allocation on increasing the PAPR is very clear especially with RU#2 and RU#3. In general, it has been found that the proposed DST-OFDMA system provides better performance over the conventional DFT-OFDMA system and a lower complexity and cost over the recent DST-SC-FDMA system.

Acknowledgment

This work is supported by Research Supporting Grant Scheme (RSGS) Vot U102 and Universiti Tun Hussein Onn Malaysia (UTHM).

References:

[1] Myung, H. G., & Goodman, D. J. Single carrier FDMA: A new air interface for long term evolution. London: Wiley (2008).

[2] Zhuang, L., Liu, L., Li, J., Shao, K. and Wang, G. Discrete Sine and Cosine Transforms in Single Carrier Modulation Systems. Wireless Pers Commun, 78(2), pp.1313-1329. (2014).

[3] Zihuai, L., Pei, X., Branka, V., &Mathini, S. Analysis of receiver algorithms for LTE SC-FDMA based uplink MIMO systems. IEEE Transactions on Wireless Communications, 9(1), 60–65. (2010).

[4] Al-kamali F.S., Dessouky M.I., Sallam B.M., Shawki F., Al-Hanafy W., Abd El-Samie F.E.: 'Joint low-complexity equalization and carrier frequency offsets compensation scheme for MIMO SC-FDMA systems', IEEE Trans. Wirel. Commun., 11, (3), pp. 869–873. (2012).

[5] Wang, G., Shao, K.,&Zhuang, L. Time-varyingmulticarrier and single-carrier modulation system. IET Signal Processing, 7, 1–12. (2013).

[6] Al-kamali F.S., Dessouky M.I., Sallam B.M., Abd El-Samie F.E., Shawki F.: 'A new single-carrier FDMA system based on the discrete cosine transform'. ICCES'9 Conf., Cairo, Egypt, 14–16 December pp. 555–560. 2009.

[7] Merched, R. On OFDM and single-carrier frequency-domain systems based on trigonometric transforms. IEEE Signal Processing Letters, 13(8), pp.473-476. (2006).

[8] Wang, Sen-Hung, et al. "A novel low-complexity precoded OFDM system with reduced PAPR." IEEE Transactions on Signal Processing 63.6 .1366-1376. (2015).

[9] Tomar, Pargtee, Mitra Sharma, and Bhawani Shankar Chaudhary. "Bit Error Rare (BER) Analysis of Conventional OFDM (DFT-OFDM) and Wavelet Based OFDM (DWT–OFDM)." International Journal on Recent and Innovation Trends in Computing and Communication 3.1 (2015): 423-426.

[10] Sorrentino, Stefano. "Methods and apparatuses for multiple access in a wireless communication network using DCT-OFDM." U.S. Patent No. 8,693,571. 8 Apr. (2014).

[11] Suma, Manuvinakurike Narasimhasastry, Somenahalli Venkatarangachar Narasimhan, and Buddhi Kanmani. "Orthogonal frequency division multiplexing peak-toaverage power ratio reduction by best tree selection using coded discrete cosine harmonic wavelet packet transform." IET Communications 8.11: 1875-1882. (2014)

[12] Fathi E. Abd El-Samie, Faisal S. Al-Kamali, Azzam Y. Al-nahari, and, Moawad I.Dessouky, SC-FDMA for Mobile Communications .CRC Press. (2013).

[13] Baig, I., Jeoti, V., Ikram, A. and Ayaz, M. PAPR reduction in mobile WiMAX: a novel DST precoding based random interleaved OFDMA uplink system. Wireless Netw, 20(5), pp.1213-1222. (2013).

[14] Al-kamali, F. New single-carrier transceiver scheme based on the discrete sine transform. The Journal of Engineering. IET JOE, pp. 1-5. (2014).

[15] Bashar ali and Nor shahidah. " IQI Problem In Discrete Sine Transform Based FDMA Systems." WSEAS TRANSACTIONS ON COMMUNICATIONS,10,292,,11092742 .(2016).

[16] Al-kamali, F. S., Hefdhallah Sakran, and N. A. Odhah. "I/Q Imbalance Problem in SC-FDMA System with DCT and DFT Basis Functions." Advances in Electrical Engineering (2015).